

ChemComm

Chemical Communications

Accepted Manuscript

This article can be cited before page numbers have been issued, to do this please use: J. Liu, X. Liao, K. Xiong, S. Kuang, C. Jin, L. Ji and H. Chao, *Chem. Commun.*, 2020, DOI: 10.1039/D0CC01148G.



This is an Accepted Manuscript, which has been through the Royal Society of Chemistry peer review process and has been accepted for publication.

Accepted Manuscripts are published online shortly after acceptance, before technical editing, formatting and proof reading. Using this free service, authors can make their results available to the community, in citable form, before we publish the edited article. We will replace this Accepted Manuscript with the edited and formatted Advance Article as soon as it is available.

You can find more information about Accepted Manuscripts in the [Information for Authors](#).

Please note that technical editing may introduce minor changes to the text and/or graphics, which may alter content. The journal's standard [Terms & Conditions](#) and the [Ethical guidelines](#) still apply. In no event shall the Royal Society of Chemistry be held responsible for any errors or omissions in this Accepted Manuscript or any consequences arising from the use of any information it contains.

Journal Name

COMMUNICATION

Boosting two-photon photodynamic therapy with mitochondria-targeting ruthenium-glucose conjugates†

 Jiangping Liu,^a Xinxing Liao,^a Kai Xiong,^a Shi Kuang,^a Chengzhi Jin,^a Liangnian Ji,^a and Hui Chao^{*ab}

 Received 00th January 20xx,
Accepted 00th January 20xx

DOI: 10.1039/x0xx00000x

www.rsc.org/

Herein we present a series of dual-targeted ruthenium-glucose conjugates that can function as two-photon absorption (TPA) PDT agents to effectively ablate tumors by preferentially targeting both tumor cells and mitochondria. The *in vivo* experiments revealed an excellent tumor inhibitory efficiency of the dual-targeted TPA PSs.

Cancer has posed a primary threat to human health. Although platinum compounds are the most broadly used anticancer drugs in the clinic, there is a critical unmet need for new generations of anticancer agents to combat chemo-resistance and reduce side effects.¹ The advent of photodynamic therapy (PDT) opens an avenue to circumvent the above concerns by virtue of its spatiotemporal selectivity and less subjection to cross resistance with existing pharmaceuticals.^{1b} In principle, PDT is based on the interactions of oxygen with non-toxic photosensitizers (PSs) under the irradiation of appropriate light which in tandem yield a highly toxic reactive oxygen species (ROS) triggering biological responses. However, the Achilles' heel for PDT lies in the insufficient dosage of the three fundamental elements (i.e., PSs, oxygen, and light) in diseased tissues.² Such defects will entail either a higher light fluence or a larger drug dosage to maintain PDT efficacy, which is very likely to incur unwanted metabolic toxicity or photothermal damages to peripheral normal tissues. These considerations indicate the urgency of developing novel PSs that is capable of targeting cancer cells as well as effectively ruining tumors.

Unlike normal cells, cancer cells are overwhelmingly fuelled by glycolysis of which the energy production efficiency is much lower than that of oxidative phosphorylation (OXPHOS) in normal cells. Hence, the uncontrolled fast growth and

proliferation of cancer cells are much more desperate for D-glucose; such obsession with D-glucose of cancer cells is known as "Warburg effect". The commonly observed overexpression of glucose transporters (GLUTs) in cancer cells are responsible for the fast D-glucose intake and have provided clinically validated targets for cancer therapy.³ The extensively deployed radiolabeled glucose derivative ¹⁸F-fluorodeoxyglucose (¹⁸F-FDG) for clinical cancer diagnosis in PET imaging⁴ corroborates the feasibility of using glucose conjugation to acquire cancer-targeting ability. Indeed, there is a growing recognition that glucose conjugation has a high likelihood to confer many compounds with an ability to target cancer.^{3e, 5} Such strategy has also been extended to biotin, folic acid, etc.⁶ Another issue to tackle is that PDT resistance arises when facing hypoxic tumors.⁷ Despite many sophisticated counterstrategies in the realm of nanomaterials^{2b}, an elegant solution to maintain efficacy for molecular PSs is to redirect the PSs to mitochondrion⁸ which plays a decisive role on the cell fate. Studies have shed light on the way to overcoming cancer resistance by undermining mitochondria homeostasis.⁹ Amongst the strategies of accessing mitochondria, taking advantage of the intrinsic affinity of some metal complexes towards mitochondrial would be an auspicious option.¹⁰ As for breaking the penetration limitation of light, TPA technique can be harnessed to great effect in PDT due to its peculiar spatial resolution and deeper tissue penetration depth in near infrared (NIR) therapeutic window.¹¹

In the arsenal of PDT, transition metal complexes emerged as promising candidates in recent decade due to their distinct appealing characteristics from the organic counterpart in both photophysical and pharmacokinetic facets. For example, many Ru(II) complexes manifested rapid systemic clearance, significant TPA property, which are favorable for PDT.¹² It's noteworthy that an inert polypyridyl Ru(II) complex (TLD1433) developed by McFarland *et al.* has reached phase IB clinical trials for PDT treatment of bladder carcinoma. Our previous work also suggested that some inert polypyridyl Ru(II) complexes hold the promise to target mitochondria and can

^a MOE Key Laboratory of Bioinorganic and Synthetic Chemistry, School of Chemistry, Sun Yat-Sen University, Guangzhou, 510275, P R China. E-mail: ceschh@mail.sysu.edu.cn

^b MOE Key Laboratory of Theoretical Organic Chemistry and Functional Molecule, School of Chemistry and Chemical Engineering, Hunan University of Science and Technology, Xiangtan, 400201, P. R. China

†Electronic supplementary information (ESI) available: Experimental details and figures referenced throughout the text. See DOI: 10.1039/x0xx00000x.

function as efficient PDT agents.^{11e} Given judicious modifications, Ru(II) complexes can be readily shaped with

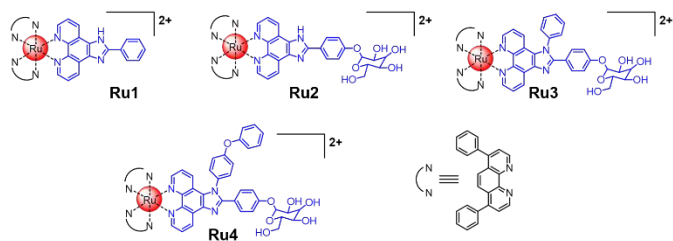


Fig. 1 Structures of Ru1-Ru4 (isolated as chloride salts)

various biological activities. With these perceptions in mind, we designed a series of Ru(II)-glucose conjugates aiming at realizing enhanced TPA PDT in tumors by a dual-targeted strategy. Herein, we present the synthesis, characterization, and in depth *in vitro* and *in vivo* tests of a series of Ru(II)-glucose conjugates (**Ru1-Ru4**, Fig. 1) as cancer cells and mitochondria dual-targeted TPA PSs. As far as we are concerned, such kind of studies with *in vivo* investigations remain very scarce and are in urgent demand.

In particular, a C1-type D-glucose conjugation was adopted to couple the Ru(II) complexes with glucose, because C1-substituted positional isomer outperforms others in mimicking the naturally occurring events during GLUTs-mediated intake and shows a higher tolerance to maintain GLUTs affinity for bulky conjugated molecules.^{3c, 3e, 5f} We envisaged such molecular engineering would minimize the influences of steric hindrance from the Ru(II) moiety and retain affinity towards GLUTs. The D-glucose fragment was fully acetylated in advance for the sake of purification, and was hydrolyzed at the end of synthesis. Detailed information for the synthesis and characterizations of **Ru1-Ru4** are documented in the Supporting Information (Scheme S1†, Fig. S1-S6†, Table S1†).

The TPA cross sections (σ_2) of **Ru1-Ru4** were determined by a well-developed TPEF method in the range of 800 nm to 880 nm. The results (shown in Fig. 2a, and Fig. S7†) revealed the maximum σ_2 of the complexes emerged at 810 nm. Of note, **Ru4** exhibited the largest σ_2 value of 181 GM ($1 \text{ GM} = 1 \times 10^{-50} \text{ cm}^2 \text{ s}^4 \text{ photon}^{-1} \text{ molecule}^{-1}$), which is well comparable to that of reported molecular TPA PSs,^{11d, 13} and is much higher than that of many reported TPA organometallic probes^{11c} and PDT prototype agents, such as tetraphenylporphyrin (H_2TTP , 2.8 GM)^{13c} and $\text{Ru}(\text{bpy})_3^{2+}$ (66 GM)^{13a}.

To determine the singlet oxygen ($^1\text{O}_2$) quantum yields (Φ_Δ) of **Ru1-Ru4**, we studied the $^1\text{O}_2$ phosphorescence intensity at 1273 nm [$^1\Delta_g \rightarrow ^3\Sigma_g^-(0, 0)$] of a **Ru1-Ru4** solution at various $\text{OD}_{450\text{nm}}$ values upon irradiation (Fig. 2b). The slope of the curve of emission intensity versus $\text{OD}_{450\text{nm}}$ revealed the Φ_Δ values of 0.74, 0.85, 0.75, and 0.90, respectively, with $[\text{Ru}(\text{bpy})_3]^{2+}$ as the reference compound, all of which outperformed H_2TTP (0.70)^{11e}. In an indirect measurement, 1,3-diphenylisobenzofuran (DPBF) was used as the $^1\text{O}_2$ indicator. The selective oxidation of DPBF by $^1\text{O}_2$ gave rise to its emission attenuation (Fig. 8†). The determined Φ_Δ values (Table S2†) are in line with the previous results. In addition, the $\Phi_\Delta \times \sigma_2$ values were utilized to estimate

the merit of the ROS generating ability of compounds in TPA PDT, where **Ru1-Ru4** showed vastly superior efficiency than H_2TTP by

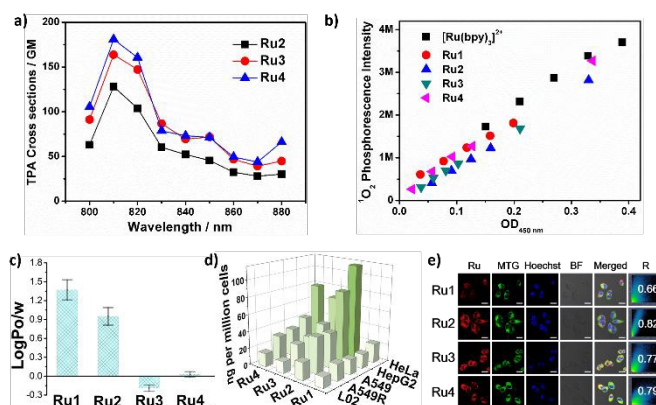


Fig. 2 (a) Two-photon absorption cross sections of **Ru2-Ru4** at different excitation wavelengths ranging from 800 nm to 880 nm. (b) Plots of integrated $^1\text{O}_2$ phosphorescence intensity versus $\text{OD}_{450 \text{ nm}}$ in the presence of **Ru1-Ru4** in aerated methanol at various concentrations. (c) Octanol/water partition coefficients of **Ru1-Ru4**, the error bars denote standard deviation calculated from three replicates. (d) ICP-MS quantification of the internalized Ru by different cell lines. Cells were treated with **Ru1-Ru4** (10 μM , 1% DMSO, v/v) in non-glucose culture medium at 37 $^\circ\text{C}$ for 2 h in the dark. (e) Confocal co-localization images of **Ru1-Ru4** (10 μM , $\lambda_{\text{ex}} = 458 \text{ nm}$, $\lambda_{\text{em}} = 600\text{-}650 \text{ nm}$), MTG ($\lambda_{\text{ex}} = 488 \text{ nm}$, $\lambda_{\text{em}} = 510\text{-}540 \text{ nm}$), and Hoechst 33342 ($\lambda_{\text{ex}} = 405 \text{ nm}$, $\lambda_{\text{em}} = 410\text{-}450 \text{ nm}$) in HeLa cells. R value represents the overlap coefficient. Inset scale bars: 20 μm .

approximately two orders of magnitude in values.

The lipophilicity of a compound exerts significant influence on its cellular intake and intracellular distribution, and can be characterized by logP. As shown in Fig. 2c, **Ru1-Ru3** showed diminishing logP values. The comparison of **Ru1** and **Ru2** suggests the inclusion of glucose moiety results in moderate lipophilicity loss. Intriguingly, the phenyl substitution in imidazole dramatically reduces the lipophilicity of **Ru3**. The stability of complexes in culture medium was examined by tracking the luminescence emission profile of the mixture over 24 hours (Fig. S9†). No obvious changes in the emission profile is observed suggesting the good stability of the complexes in biological conditions. To verify our cancer selectivity assumption, we tested the cellular uptake of the complexes in various cancer cell lines (cervical cancer HeLa cell line, liver hepatocellular carcinoma HepG2 cell line, human pulmonary carcinoma A549 cell line and cisplatin resistant A549R cell line) as well as human hepatic L02 cell line under the circumstance of glucose starvation to mimic the deprivation of glucose in tumor microenvironment shaped by the chaotic vascularization, diffusion limit and fast glucose consumption.¹⁴ As shown in Fig. 2d and Table S3†, wide discrepancies in the uptake dosage of **Ru2-Ru4** were observed between different cell lines among which L02 exhibited the lowest uptake level whereas HeLa cells showed the supreme uptake level. In sharp contrast, **Ru1** which contains no glucose scaffold barely showed difference between L02 and cancer cell lines. These findings strongly suggest the involvement of GLUTs in the uptake process. Moreover, the uptake of **Ru2** evidently excelled other compounds in every cancer cell line, which can be tentatively attributed to its superior structural affinity for GLUTs over others. To

corroborate these findings, an uptake study of **Ru2** in HeLa/L02 mixed cells were conducted on a confocal laser scanning microscope (CLSM). As shown in Fig. 10 †, under identical incubation conditions HeLa cells manifested obviously stronger Ru(II) luminescence intensity than L02, suggesting the higher uptake efficiency of HeLa cells over L02 cells, which is in accordance with previous experiment. These results combined led us to the conclusion that the inclusion of D-glucose to Ru(II) complexes had endowed the conjugates with a property to preferential accumulate in cancer cells.

The distinct intake level between cancerous and normal cells enticed a comparison uptake mechanism study of **Ru1** and **Ru2** on a CLSM. It's been clear that D-glucose uptake can be mediated by two manners: (i) by GLUTs in an energy-independent facilitative diffusion process; (ii) by sodium-dependent glucose cotransporters (SGLTs) in an energy-dependent active transport process.^{3c, 3f} As shown in the results (Fig. 11 †), the uptake of **Ru2** decreased by almost the same percentage (ca. 80%) in the presence of either metabolic inhibitors or phlorizin which is an SGLTs inhibitor, suggesting that the SGLTs were probably the sole contributor for active transport which made up the majority of the total uptake. Nevertheless, the incomplete uptake inhibition by phlorizin/metabolic inhibitors compared to the 4°C group explicitly indicated the existence of a small proportion (ca. 20%) of energy-independent manners which can be attributed to GLUTs-mediate diffusion or passive diffusion. In contrast, the translocation of **Ru1** into cells is independent of energy and various transporters. Therefore, it is reasonable to deduce that **Ru1** crossed the plasma membrane by passive diffusion whereas **Ru2** primarily by a glucose transporter-mediated manner. Therefor the results thus far have confirmed our assumption of achieving cancer cell selectivity with the aid of cancer cell specific overexpressed glucose transporters.

In order to study their intracellular distributions, a co-localization study with MitoTracker green (MTG) and Hoechst 33342 was performed by CLSM in HeLa cells. As shown in Fig. 2e, the majority of **Ru1-Ru4** were in cytosol and very few entered nucleus. The complexes accumulated in mitochondria to varying degrees with overlap coefficients (R) ranging from 0.66 to 0.82. Among them **Ru2** showed the best superimposition patterns between MTG and the Ru channel with the highest R value of 0.82. Such phenomenon is in agreement with the mitochondrial characteristic of sponge-like intake for lipophilic cations. To quantify the intracellular distribution, we conducted an ICP-MS experiment under identical incubation conditions to co-localization study. The results are shown in Fig. S12 † and Table S4 †. **Ru2-Ru4** was concentrated in the mitochondria by more than 81% whereas **Ru1** by approximately 70%. Both experiments suggest that these complexes can accumulate in mitochondria. These findings set the stage for the dual-targeted therapeutics.

Since mitochondrial dysfunction can readily take place when a bulky dosage of PSs reside inside, we assessed the mitochondria membrane potential (MMP) changes of HeLa cells (Fig. S13 †) by JC-1 staining after the administration of **Ru1-Ru4** for 22 h in the dark. Surprisingly, HeLa cells treated with Ru(II)

compounds showed no appreciable MMP reductions in comparison with controls. Moreover, an apparent activation of caspase-3/7 was observed in post-PDT (450 nm, 12 J/cm²) HeLa cells, whereas no obvious difference can be found without PDT (Fig. S14 †). Taken together, the results revealed the low dark toxicity and mitochondrial destruction potency of **Ru1-Ru4** in PDT.

A toxicity experiment on various cell lines was carried out to assess the PDT efficacy *in vitro* with a mild light fluence at 450 nm (12 J/cm²) and the IC₅₀ values are summarized in Table S5 †. H₂TPP, a prototype of clinically used PDT agents, was used for comparison. As we can see, **Ru1-Ru4** showed very low lethality in the absence of irradiation. In contrast, the toxicity increased dramatically after PDT treatment. Meanwhile, the PDT lesions towards cancerous cell lines are appreciably stronger than towards L02 cell line. These findings unclosed the selectively enhanced PDT potency of **Ru2-Ru4**. The discriminative toxicity between **Ru1** and **Ru2-4** towards cancerous cell lines can be attributed to the distinct cellular intake levels. **Ru2** demonstrated the most efficient PDT efficacy in cancerous cells with a PI value of 44 in HeLa cells, which may be explained by its best mitochondrial location and uptake level. In view of this, we used **Ru2** as candidate compound for TPA PDT and *in vivo* evaluations.

Since we have discussed the feasibility of **Ru2** for TPA-induced ROS generation, we used dichlorofluorescein diacetate (DCFH) as a ROS indicator to further evaluate the *in vitro* generation of ROS under two-photon excitation. As shown in Fig. 3a, there was a significant increase in the DCF fluorescence intensity in HeLa cells treated with **Ru2** upon two-photon laser irradiation (25 mW, 120 s), and blebs formation was observed, while cells of the control group showed no obvious fluorescence or morphology changes. These disparities suggesting the TPA PDT efficacy of **Ru2** under a safe two-photon laser power. The TPA PDT procedure was studied under a closer scrutiny by annexin V-fluorescein isothiocyanate (AV) / propidium iodide (PI) co-staining and imaging on a CLSM. The results (Fig. 3b and Fig. S15 †) reconfirmed the safe fluence of laser and the integrity loss of HeLa cells administrated with **Ru2** in TPA PDT.

The excellent *in vitro* PDT properties of **Ru2** prompted further *in vivo* investigation. BALB/c mice bearing HeLa tumor

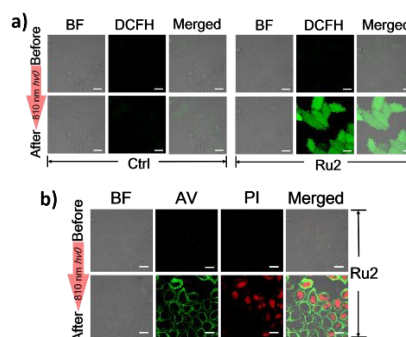


Fig. 3 (a) Confocal fluorescence images of the HeLa cells stained with DCFH ($\lambda_{\text{ex}} = 488$ nm, $\lambda_{\text{em}} = 515\text{-}540$ nm) followed by the incubation of **Ru2** (10 μM) and culture medium (Ctrl), respectively, before and after TPA PDT at 810 nm (25 mW, 120 s). (b) Annexin V/PI co-staining of the HeLa cells before and after TPA PDT (annexin V: $\lambda_{\text{ex}} = 488$ nm, $\lambda_{\text{em}} = 510\text{-}535$ nm; PI: $\lambda_{\text{ex}} = 536$ nm, $\lambda_{\text{em}} = 600\text{-}630$ nm) at 810 nm (25 mW, 120 s). Cells were

preloaded with Ru2 (10 μ M) and stained with annexin V/PI before the irradiation. Inset scale bars represent 20 μ m.

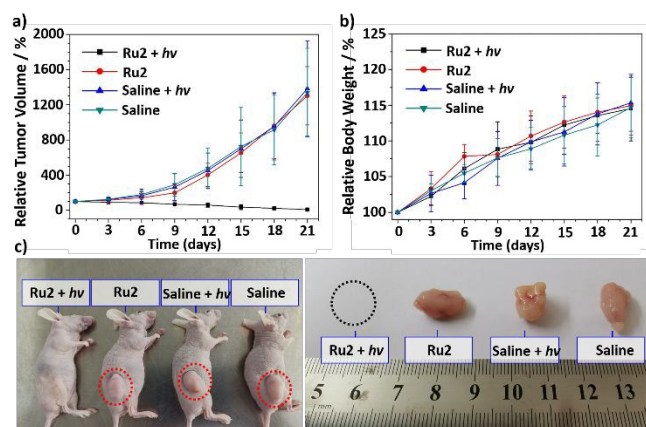


Fig. 4 (a) Tumor growth curves recorded by tumor volume change. (b) Average body weight of tumor-bearing mice. (c) Representative photographs of HeLa tumors in mice for four different treatments.

xenograft were used as the *in vivo* model. The mice were randomly divided into four groups (6 mice/group) before the experiment (day 0) and treated with: (i) Ru2 followed by two-photon irradiation; (ii) Ru2; (iii) Saline followed by two-photon irradiation; (iv) Saline. For group (i) and (iii), the TPA PDT (25 mW, 120 s) commenced 2 h after the intravenous injection of therapeutic agents. Tumor volume and mice weight were recorded every 3 days. The whole PDT therapeutic regimen comprised three identical courses, each lasted for 7 days. As shown in Fig. 4a, tumors in group (i) gradually shrank and ultimately disappeared, while those in other group grew by more than 12-fold larger in volume compared to the origin over the same period. In addition, no appreciable body weight loss was observed in the experimental groups (Fig. 4b). On the contrary, the weight grew by 15% at the end of the regimen, indicating the side effect from the drug and light fluence are well tolerant. Under closer scrutiny of the H&E staining of the sections of major organs as well as tumors (Fig. S16[†]), we reconfirmed compound Ru2 is void of noticeable side effects towards mice. The eradication of tumor in group (i) strongly indicates the effective *in vivo* TPA PDT efficacy of Ru2. This can be attributed to not only the excellent photophysical properties of Ru2, but also the mitochondria-targeted lesion as well as multi-course treatment which allows tumors to replenish oxygen incurring higher PDT efficacy in the context of hypoxia.

In summary, we have prepared a series of dual-targeted Ru(II)-glucose conjugates that can preferentially accumulate in both cancer cells and mitochondria, and effectively exert TPA PDT efficacy. In particular, Ru2 which showed the best *in vitro* PDT performance and was capable of subduing tumors *in vivo* is a promising candidate for cancer-specific TPA PDT.

This work was supported by the National Science Foundation of China (Nos. 21807119, 21778079, 21525105), Natural Science Foundation of Guangdong Province (No. 2020A1515011153), the Fundamental Research Funds for the Central Universities (No. 19lgpy132), and the Ministry of Education of China (No. IRT-17R111).

Conflicts of interest

There are no conflicts to declare.

References

- (1) H. Huang, S. Banerjee, K. Qiu, P. Zhang, O. Blacque, T. Malcomson, M. J. Paterson, G. J. Clarkson, M. Staniforth, V. G. Stavros, G. Gasser, H. Chao, P. J. Sadler, *Nat. Chem.*, 2019, doi.org/10.1038/s41557-019-0328-4; (2) C. Imberti, P. Zhang, H. Huang, P. J. Sadler, *Angew. Chem. Int. Ed.*, 2020, **59**, 61.
- (a) J. Liu, C. Zhang, T. W. Rees, L. Ke, L. Ji, H. Chao, *Coordin. Chem. Rev.*, 2018, **363**, 17; (b) W. Fan, P. Huang, X. Chen, *Chem. Soc. Rev.*, 2016, **45**, 6488.
- (a) R. A. Gatenby, R. J. Gillies, *Nat. Rev. Cancer*, 2004, **4**, 891; (b) M. L. Macheda, S. Rogers, J. D. Best, *J. Cell. Physiol.*, 2005, **202**, 654; (c) M. Patra, S. G. Awuah, S. J. Lippard, *J. Am. Chem. Soc.*, 2016, **138**, 12541; (d) Y. Tian, H. Lee, C. Lim, J. Park, H. Kim, Y. Shin, E. Kim, H. Jeon, S. Park, B. Cho, *Angew. Chem. Int. Ed.*, 2009, **48**, 8027; (e) E. C. Calvaresi, P. J. Hergenrother, *Chem. Sci.*, 2013, **4**, 2319; (f) M. B. Calvo, A. Figueroa, E. G. Pulido, R. G. Campelo, L. A. Aparicio, *Int. J. Endocrinol.*, 2010, **2010**, 205357.
- C. Plathow and W. A. Weber, *J. Nucl. Med.*, 2008, **49 Suppl 2**, 43S.
- (a) M. L. Bowen, C. Orvig, *Chem. Commun.*, 2008, 5077; (b) T. C. Johnstone, K. Suntharalingam, S. J. Lippard, *Chem. Rev.*, 2016, **116**, 3436; (c) P. Liu, Y. Lu, X. Gao, R. Liu, D. Zhang-Negrerie, Y. Shi, Y. Wang, S. Wang, Q. Gao, *Chem. Commun.*, 2013, **49**, 2421; (d) M. Louie, H. Liu, M. Lam, Y. Lam, K. K. Lo, *Chem. Eur. J.*, 2011, **17**, 8304; (e) M. Gottschaldt, U. S. Schubert, S. Rau, S. Yano, J. G. Vos, T. Kroll, J. Clement, I. Hilger, *ChemBioChem*, 2010, **11**, 649; (f) Y. Cheng, G. Shabir, X. Li, L. Fang, L. Xu, H. Zhang, E. Li, *Chem. Commun.*, 2020, **56**, 1070.
- (a) H. Wang, J. Chang, M. Shi, W. Pan, N. Li, B. Tang, *Angew. Chem. Int. Ed.*, 2019, **58**, 1057; (b) R. Zhao, B. Wang, X. Yang, Y. Xiao, X. Wang, C. Shao, R. Tang, *Angew. Chem. Int. Ed.*, 2016, **55**, 5225; (c) K. Co, G. Li, C. Leung, D. Ma, *Coordin. Chem. Rev.*, 2019, **381**, 79; (d) T. Wang, N. Zabarska, Y. Wu, M. Lamla, S. Fischer, K. Monczak, D. Y. W. Ng, S. Rau, T. Weil, *Chem. Commun.*, 2015, **51**, 12552.
- B. A. Teicher, *Cancer Metast Rev.*, 1994, **13**, 139.
- W. Lv, Z. Zhang, K. Zhang, H. Yang, S. Liu, A. Xu, S. Guo, Q. Zhao, W. Huang, *Angew. Chem. Int. Ed.*, 2016, **55**, 9947.
- R. C. H. Robin, A. J. Smith, M. P. Murphy, *Antioxid. Redox Sign.*, 2011, **15**, 3021.
- (a) Y. Chen, T. W. Rees, L. Ji, H. Chao, *Curr. Opin. Chem. Biol.*, 2018, **43**, 51; (b) S. Imstepf, V. Pierroz, R. Rubbiani, M. Felber, T. Fox, G. Gasser, R. Alberto, *Angew. Chem. Int. Ed.*, 2016, **55**, 2792; (c) A. T. Hoye, J. E. Davoren, P. Wipf, M. P. Fink, V. E. Kagan, *Acc. Chem. Res.*, 2008, **41**, 87.
- (a) Z. Zhou, J. Liu, J. Huang, T. W. Rees, Y. Wang, H. Wang, X. Li, H. Chao, P. J. Stang, *Proc. Natl. Acad. Sci. U. S. A.*, 2019, **116**, 20296; (b) Z. Zhou, J. Liu, T. W. Rees, H. Wang, X. Li, H. Chao, P. J. Stang, *Proc. Natl. Acad. Sci. U. S. A.*, 2018, **115**, 5664; (c) Y. Chen, R. Guan, C. Zhang, J. Huang, L. Ji, H. Chao, *Coordin. Chem. Rev.*, 2016, **310**, 16; (d) L. K. McKenzie, H. E. Bryant, J. A. Weinstein, *Coordin. Chem. Rev.*, 2019, **379**, 2; (e) J. Liu, Y. Chen, G. Li, P. Zhang, C. Jin, L. Zeng, L. Ji, H. Chao, *Biomaterials*, 2015, **56**, 140.
- F. Heinemann, J. Karges, G. Gasser, *Acc. Chem. Res.*, 2017, **50**, 2727.
- (a) H. Huang, B. Yu, P. Zhang, J. Huang, Y. Chen, G. Gasser, L. Ji, H. Chao, *Angew. Chem. Int. Ed.*, 2015, **54**, 14049; (b) J. Liu, C. Jin, B. Yuan, Y. Chen, X. Liu, L. Ji, H. Chao, *Chem. Commun.*, 2017, **53**, 9878.
- C. Carmona-Fontaine, V. Bucci, L. Akkari, M. Deforet, J. A.

Journal Name

COMMUNICATION

Joyce, J. B. Xavier, *Proc. Natl. Acad. Sci. USA.*, 2013, **110**, 19402.

View Article Online
DOI: 10.1039/D0CC01148G